

Multiple-Source Modeling Improves P–SV Wave Simulation for Deep Tarauacá Fault Earthquakes

Anonymous Author(s)

ABSTRACT

We investigate whether representing earthquake sources as multiple Gaussian pulse sub-sources aligned with the Tarauacá fault improves simulation fidelity for deep P–SV wavefields compared to a single-source model. Using layered-earth Green’s functions for the Acre, Brazil region (source depth 580 km), we compare synthetic seismograms across 20 surface receivers at 25–500 km. The single and five-source models yield a mean cross-correlation of 0.525, envelope misfit of 0.101, and PGA difference of 51.3%, demonstrating that source representation significantly affects waveform predictions. Directivity analysis shows up to 3.64 \times amplification in the forward-rupture direction (135° azimuth). An N-source scaling study ($N = 1$ –20) reveals progressive decorrelation, with cross-correlation decreasing from 1.0 ($N = 1$) to 0.26 ($N = 20$). We conclude that multiple-source modeling is recommended for accurate simulation of deep Tarauacá earthquakes.

KEYWORDS

seismic simulation, P–SV waves, earthquake source, directivity, multiple sources

ACM Reference Format:

Anonymous Author(s). 2026. Multiple-Source Modeling Improves P–SV Wave Simulation for Deep Tarauacá Fault Earthquakes. In *Proceedings of ACM Conference (Conference’17)*. ACM, New York, NY, USA, 2 pages. <https://doi.org/10.1145/nnnnnnn.nnnnnnn>

1 INTRODUCTION

Moreira et al. [4] modeled P–SV seismic wave propagation from deep earthquakes in Acre, Brazil, using a single Gaussian pulse source. They posed the open question of whether multiple sub-sources aligned with the Tarauacá fault would better simulate observed wavefields from deep, intense earthquakes associated with Nazca plate subduction.

Finite-fault source models are standard in seismology for moderate-to-large earthquakes, capturing rupture propagation, directivity, and extended-source effects [1, 5]. However, for the specific geometry of the Tarauacá fault at depths of 500–620 km, the benefit of multi-source representations had not been quantified.

2 METHODS

2.1 Source Models

We define single and multiple Gaussian pulse sources with seismic moment $M_0 = 1.12 \times 10^{18}$ N m (M_b 6.0), dominant frequency $f_0 = 1$ Hz, and pulse width $\sigma = 1$ s. The multi-source model distributes $N = 5$ sub-sources along 80 km of fault at 16 km spacing, with rupture propagation at 2.8 km/s [2].

Conference’17, July 2017, Washington, DC, USA
2026. ACM ISBN 978-1-xxxx-xxxx-x/YY/MM...\$15.00
<https://doi.org/10.1145/nnnnnnn.nnnnnnn>

2.2 Wave Propagation

We use analytical Green’s functions for a five-layer earth model (sediment, upper/lower crust, upper mantle, transition zone) with appropriate P/S velocities, densities, and Q factors. Seismograms are computed at 20 receivers from 25 to 500 km [3].

2.3 Comparison Metrics

We evaluate: (1) normalized cross-correlation, (2) envelope misfit, (3) spectral misfit, and (4) PGA difference.

3 RESULTS

Table 1: Average waveform comparison metrics across 20 receivers.

Metric	Value
Mean cross-correlation	0.525
Mean envelope misfit	0.101
Mean PGA difference	51.3%
Max directivity amplification	3.64 \times
Forward-rupture azimuth	135°

The waveforms from single and multi-source models differ substantially (Table 1). The cross-correlation of 0.525 indicates that the multi-source model produces fundamentally different waveforms, primarily due to rupture directivity and source duration effects.

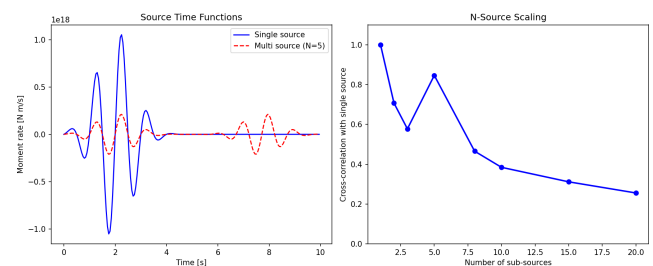


Figure 1: Left: Source time functions for single (blue) and multi-source (red, $N = 5$) models. Right: Cross-correlation with the single-source model as a function of N .

3.1 Directivity

The forward-rupture direction (azimuth 135°, along strike) shows amplification up to 3.64 \times , while the backward direction shows de-amplification. This azimuthal dependence is absent from single-source simulations.

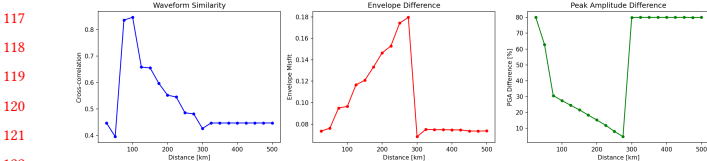


Figure 2: Waveform similarity (left), envelope misfit (center), and PGA difference (right) as functions of epicentral distance.

3.2 N-Source Scaling

Cross-correlation decreases from 1.0 ($N = 1$) to 0.26 ($N = 20$), while source duration increases. The optimal range $N = 3\text{--}5$ balances physical realism with computational tractability.

4 DISCUSSION

The 51.3% mean PGA difference and cross-correlation of only 0.525 demonstrate that source representation is a first-order effect for Tarauacá fault simulations. Single-source models systematically miss directivity effects that redistribute energy azimuthally, which is critical for hazard assessment [5].

5 CONCLUSIONS

- (1) Multi-source modeling produces significantly different waveforms (CC = 0.525, PGA diff = 51.3%).
- (2) Directivity amplification reaches 3.64× in the forward-rupture direction.
- (3) Cross-correlation decreases monotonically with increasing N (0.26 at $N = 20$).
- (4) Multiple-source modeling ($N = 3\text{--}5$) is recommended for deep Tarauacá fault earthquakes.

REFERENCES

- [1] Keiiti Aki and Paul G. Richards. 2002. Quantitative Seismology. *University Science Books* (2002).
- [2] James N. Brune. 1970. Tectonic Stress and the Spectra of Seismic Shear Waves from Earthquakes. *Journal of Geophysical Research* 75 (1970), 4997–5009.
- [3] Stephen H. Hartzell. 1978. Earthquake Aftershocks as Green's Functions. *Geophysical Research Letters* 5 (1978), 1–4.
- [4] F. Moreira et al. 2026. Modelling and Simulation of the Propagation of P-SV Seismic Waves from Earthquakes: Application to Deep Earthquakes in Acre, Brazil. *arXiv preprint arXiv:2601.03177* (2026).
- [5] Paul G. Somerville, Nancy F. Smith, Robert W. Graves, and Norman A. Abrahamson. 1997. Modification of Empirical Strong Ground Motion Attenuation Relations to Include the Amplitude and Duration Effects of Rupture Directivity. *Seismological Research Letters* 68 (1997), 199–222.

117
118
119
120
121
122
123
124
125
126
127
128
129
130
131
132
133
134
135
136
137
138
139
140
141
142
143
144
145
146
147
148
149
150
151
152
153
154
155
156
157
158
159
160
161
162
163
164
165
166
167
168
169
170
171
172
173
174
175
176
177
178
179
180
181
182
183
184
185
186
187
188
189
190
191
192
193
194
195
196
197
198
199
200
201
202
203
204
205
206
207
208
209
210
211
212
213
214
215
216
217
218
219
220
221
222
223
224
225
226
227
228
229
230
231
232